ACS APPLIED MATERIALS & INTERFACES
RESEARCH ARTICLE
www.acsami.org

A ZnO-Nanowire Phototransistor Prepared on Glass Substrates

W. Y. Weng,[†] S. J. Chang,[†] C. L. Hsu,[‡] and T. J. Hsueh[*,§]

[†]Institute of Microelectronics and Department of Electrical Engineering, Center for Micro/Nano Science and Technology, Advanced Optoelectronic Technology Center, National Cheng Kung University, Tainan 701, Taiwan

[‡]Department of Electronic Engineering, National University of Tainan, Tainan 700, Taiwan

[§]National Nano Device Laboratories, Tainan 741, Taiwan

ABSTRACT: The fabrication of a phototransistor via the bridging of two prefabricated electrodes with a laterally grown ZnO nanowire is reported. It was found that the fabricated device is an *n*-channel enhancement-mode phototransistor with a dark carrier concentration of 6.34×10^{17} cm^{-3} when the gate voltage is biased at 5 V. With an incident-light wavelength of 360 nm and a zero gate bias, it was found that the noise equivalent power and normalized detectivity (D^*) of the fabricated ZnO phototransistor were 6.67×10^{-17} W and 1.27×10^{13} cm Hz$^{0.5}$ W^{-1}, respectively. It was also found that the current in the device can be modulated efficiently by tuning the wavelength of the excitation source.

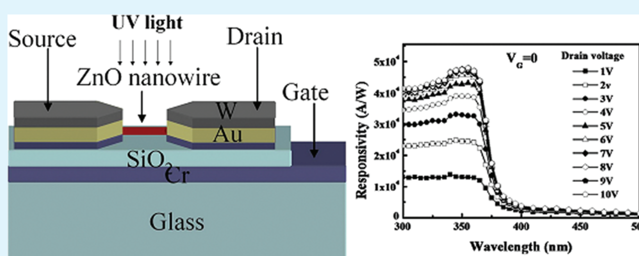

KEYWORDS: ZnO, nanowires, lateral growth, phototransistor

I. INTRODUCTION

ZnO is a chemically and thermally stable n-type semiconductor that is regarded as being potentially useful in the ultraviolet (UV) spectral region.[1,2] Two-dimensional (2D) ZnO films have been used in various applications, such as pyroelectric devices,[3] transistors,[4] piezoelectric devices,[5] surface acoustic wave devices,[6] and photodetectors.[7] Recently, 2D ZnO-based phototransistors have also been demonstrated.[8]

As an alternative to 2D films, one-dimensional (1D) nanomaterials have attracted a lot of attention because of their potential applications in nanodevices. The growth and material properties of 1D ZnO nanowires have been studied extensively. 1D ZnO-nanowire-based devices, such as light-emitting diodes,[9] transistors,[10] lasers,[11] and UV photodetectors,[12,13] have been demonstrated.

To realize practical 1D ZnO-nanowire-based devices, good contacts are required on both ends of the nanowires. The most commonly used method is to place the nanowires at proper sites and then use either electron-beam lithography or focused ion-beam deposition to form the contacts. However, these methods require tedious and time-consuming processing steps, and their production yields are low. It is also possible to form contacts by growing lateral ZnO nanowires across two prefabricated electrodes. For example, Lee et al. etched Si(110) wafers to form trenches and then grew lateral ZnO nanowires to bridge the two exposed Si(111) vertical planes.[14] For planar device applications, Law et al. demonstrated that a growth barrier can be used to suppress vertical growth, resulting in only laterally grown ZnO nanowires on the oxidized Si substrate.[15] In the present study, we report the use of a growth barrier for suppressing the vertical growth of ZnO nanowires on a glass substrate and the bridging of two prefabricated contact electrodes by a single laterally grown ZnO nanowire. The proposed method is simple, cost-effective, and suitable for mass production. A lateral-ZnO-nanowire-based UV phototransistor, which is potentially useful in space communications, ozone layer monitoring, and flame detection, is demonstrated. With the same device structure, the ZnO-nanowire phototransistor can be integrated with ZnO-nanowire field-effect transistors to realize feasible nanoscale ZnO-based optoelectronic integrated circuits. The growth of the lateral ZnO nanowire and the electrooptical properties of the fabricated phototransistor are also discussed.

II. EXPERIMENTS

Figure 1 schematically depicts the proposed ZnO-nanowire phototransistor. Prior to the growth of the ZnO nanowire, a 300-nm-thick Cr layer and a 200-nm-thick SiO_2 layer were deposited onto a glass substrate as the bottom gate electrode and insulator, respectively, by radio-frequency sputtering. A 5-nm-thick Cr layer and a 200-nm-thick Au layer were subsequently deposited onto the SiO_2 layer by electron-beam evaporation to serve as the source and drain contacts of the transistor, respectively. A 70-nm-thick W layer was then deposited by sputtering to serve as the growth barrier of vertical ZnO nanowires.[16] Photolithography and lift-off were then performed to define the source and drain contact electrodes. We then placed the patterned glass substrate and 99.9% pure zinc metal powder into an alumina boat, which was then inserted into a quartz tube to grow the ZnO nanowires. Evaporation was carried out in the quartz tube in

Received: August 17, 2010
Accepted: December 23, 2010
Published: January 12, 2011

ACS Publications © 2011 American Chemical Society

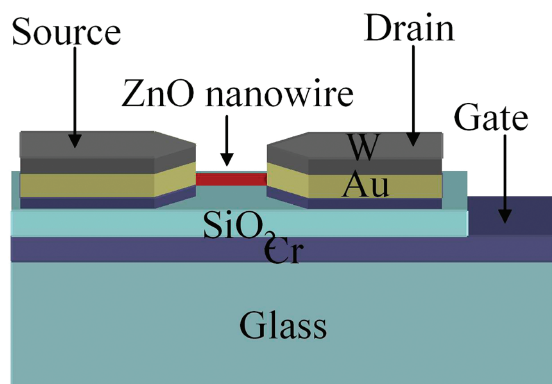

Figure 1. Schematic diagram of the proposed ZnO-nanowire phototransistor.

a horizontal tubular furnace. The diameter and length of the quartz tube were 5 and 70 cm, respectively. Argon and oxygen gases were then introduced into the furnace. It should be noted that the positions of the substrate, the zinc metal powder, and the alumina boat were carefully controlled to make them at the same horizontal level and heated to the same temperature. A mechanical pump was then used to evacuate the system, and a programmable temperature controller was used to precisely control the temperature of the furnace. The growth pressure was maintained at 10 Torr, and the growth time was 60 min. With proper control of the growth parameters, we were able to laterally grow ZnO nanowires on the Au sidewall. We designed 144 pairs of Au electrodes on the mask. However, we only successfully fabricated five working transistors with a single ZnO nanowire bridging the electrodes. To improve the production yield, we will need to further optimize the growth parameters.

A JEOL JSM-7000F field-emission scanning electron microscope operated at 10 keV was used to characterize the structural properties of the nanowires. Current−voltage ($I-V$) characteristics of the fabricated devices were then measured by an HP 4156 semiconductor parameter analyzer at room temperature. Spectral responsivity measurements of the phototransistor were performed using a Jobin-Yvon SPEX system with a 300-W Xe-arc-lamp light source (PerkinElmer PE300BUV) and a standard synchronous detection scheme.

III. RESULTS AND DISCUSSION

Figure 2 shows a top-view scanning electron microscopy (SEM) micrograph of the ZnO nanowires prepared on the patterned substrate. With the W growth barrier, it was found that no vertical ZnO nanowires grew on top of the Cr/Au/W electrodes. It was also found that ZnO nanowires can only be grown laterally from the sidewalls of the Au layer. The inset in Figure 2 shows an enlarged SEM image. It can be seen that a single laterally grown ZnO nanowire bridged the two contact electrodes to provide an electrical path. The length and diameter of the ZnO nanowire are around 1.2 μm and 60 nm, respectively.

Figure 3a shows room-temperature drain current−drain voltage (I_D-V_D) characteristics of the device measured in the dark. The transistor exhibits excellent saturation and pinch-off characteristics, indicating that the entire channel region under the gate metal can be completely depleted. When the source is grounded and the drain is positively biased, electrons are locally depleted near the drain. Similar to conventional 2D transistors, this results in pinch-off and clear saturation. Figure 3b shows the saturation drain current, I_{DSat}, as a function of the gate voltage, V_G. The on/off ratio of the fabricated transistor is over 10^4. However, we also observed a dull slope in the transfer characteristic

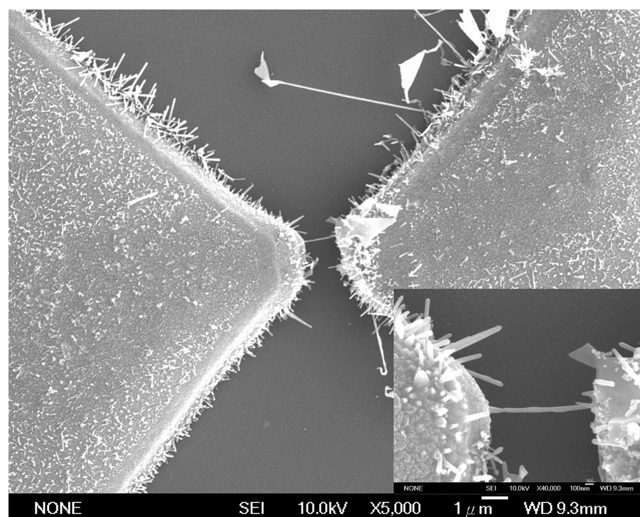

Figure 2. Top-view SEM micrograph of the ZnO nanowires prepared on a patterned substrate.

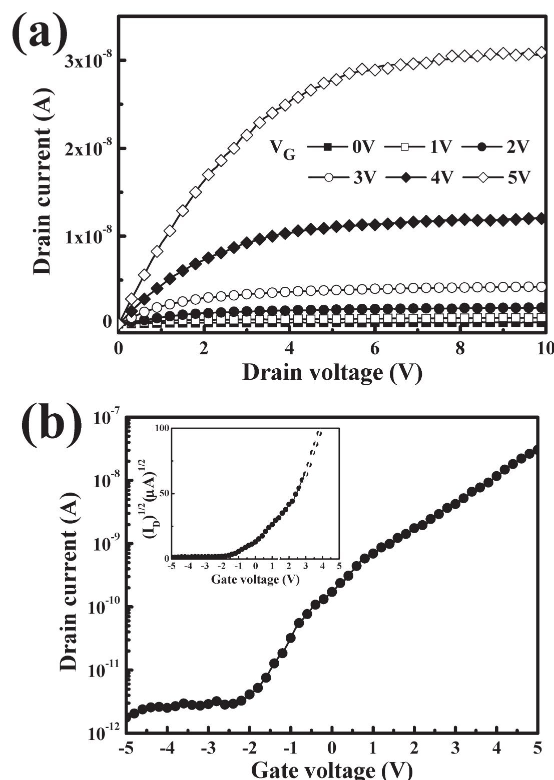

Figure 3. (a) I_D-V_D characteristics of the device measured in the dark at room temperature and (b) measured $I_{DSat}-V_G$ relationship.

and an exponential increase in I_D. The poor transfer characteristic of the ZnO device is attributed to the increased chemisorption on the ZnO-nanowire channel. Similar results have been previously reported.[17] To achieve a better transfer characteristic, we might need to deposit a passivation layer, such as SiO_2, on the surface of the ZnO nanowire.

The inset in Figure 3b shows the relationship between the drain current $I_D^{1/2}$ and the applied gate voltage. The threshold voltage, V_{th}, of the fabricated device was 1.4 V, which indicates that the fabricated device was an enhancement-mode transistor. With a

fixed gate voltage, V_G, we can determine the total charge:

$$Q_{tot} = C_g|V_G - V_{th}| \quad (1)$$

where C_g is the gate capacitance and V_{th} is the threshold voltage required to deplete the nanowire. The gate capacitance C_g can be estimated using a model of a cylinder on an infinite metal plate:[18]

$$\frac{C_g}{L} = \frac{2\pi\varepsilon_r\varepsilon_0}{\cosh^{-1}(1 + h/r)} \quad (2)$$

where r is the nanowire radius (30×10^{-7} cm), L is the nanowire channel length (1.2×10^{-4} cm), h is the SiO_2 thickness (200 nm), and ε_r (3.9) is the relative dielectric constant of SiO_2. From eq 2, C_g is around 9.55×10^{-17} F. It should be noted that the lateral ZnO nanowire was grown from the Au sidewall and that there exists a 5-nm air gap between the nanowire and SiO_2. Because the capacitance of the air gap is significantly larger than that of SiO_2, we can neglect the capacitive effect of the air gap. Knowing the total charge, Q_{tot}, we can determine the carrier concentration using

$$n_e = \frac{Q_{tot}}{e\pi r^2 L} \quad (3)$$

With a gate voltage of 5 V, it was found that the carrier concentration in the ZnO nanowire is around 6.34×10^{17} cm^{-3}. We can also estimate the electron mobility (μ) from the channel conductance (g_m) using[18]

$$u = \frac{g_m L^2}{C_g V_D} \quad (4)$$

From eq 4, the electron mobility is around 0.72 cm^2 V^{-1} s^{-1} at V_D = 1 V. The small mobility of the fabricated ZnO-nanowire transistor can be attributed to chemisorption on the ZnO-nanowire channel, which can be improved by using a proper surface passivation layer.[17]

Figure 4a shows room-temperature spectral responses of the fabricated ZnO-nanowire phototransistor using a 300-W Xe arc lamp dispersed by a monochromator as the excitation source. During the measurements, the monochromatic light, calibrated with a UV-enhanced Si diode and an optical power meter, was modulated by a mechanical chopper and collimated onto the front side of the fabricated devices using an optical fiber. The photocurrent was then recorded by a lock-in amplifier. Knowing the light power density of the various light wavelengths and the illuminated area of the ZnO nanowire, the responsivities of the phototransistor can be determined. As shown in Figure 4a, a sharp cutoff occurred at ~360 nm. It was also found that the transition region of the fabricated phototransistor was only 30 nm. This value is significantly smaller than that observed for a previously reported vertical ZnO-nanowire photodetector, probably because of elimination of the coating layer.[19] With an incident-light wavelength of 360 nm and a 1 V drain voltage bias, the measured responsivity was 1.29×10^4 A W^{-1}. When the bias voltage was increased to 10 V, the measured responsivity increased to 4.7×10^4 A W^{-1}. The significant increase in the responsivity suggests that the sample has a photoconductive gain.[20] We can also calculate the photoconductive gain of the fabricated phototransistor from the measured spectral response using

$$R = \frac{I_p}{P_{opt}} = \eta\left(\frac{q\lambda}{hc}\right)G \quad (5)$$

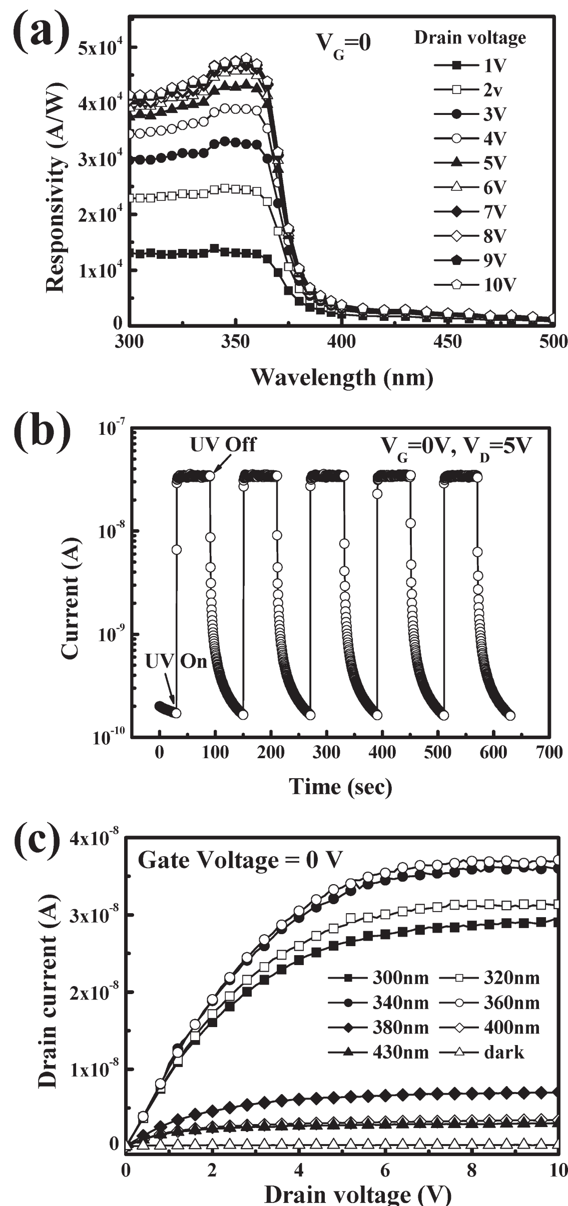

Figure 4. (a) Photocurrent measured at room temperature with V_G = 0 V and various drain voltages. (b) Transient response of the fabricated phototransistor with the UV excitation switched on and off. (c) $I_D - V_D$ characteristics of the device measured under illumination from the dispersed Xe arc lamp with a zero gate bias.

where I_p is the photocurrent, P_{opt} is the incident optical power, η is the quantum efficiency, h is Planck's constant, c is the speed of light, λ is the incident-light wavelength, and G is the photoconductive gain. Using this equation and assuming η = 1, it was found that the 4.7×10^4 A W^{-1} responsivity measured at 360 nm corresponds to a photoconductive gain of 1.62×10^5.

It is known that photoconduction of ZnO nanowires is governed by desorption and adsorption of oxygen.[21] In the dark, oxygen molecules on the surface of the nanowires carry negative charges by capturing free electrons from the n-type ZnO, creating a depletion layer with low conductivity near the surface. UV light absorption generates electron−hole pairs. The photogenerated holes oxidize the adsorbed negatively charged oxygen ions on the surface, while the remaining electrons in the conduction band increase the

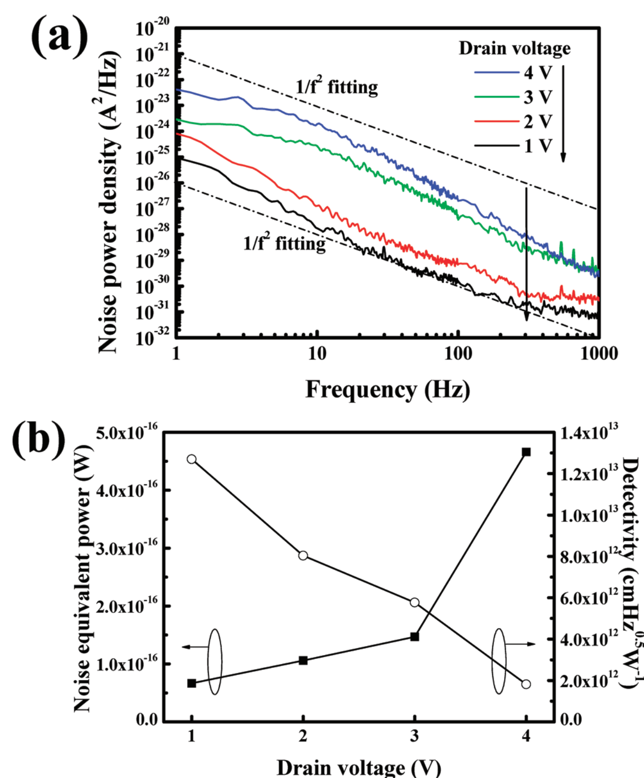

Figure 5. (a) Measured noise power spectra of the fabricated ZnO-nanowire phototransistor with various applied biases and (b) NEP and D^* values of the fabricated device.

conductivity. These oxygen-related hole-trap states at the nanowire surface prevent charge-carrier recombination and prolong the photocarrier lifetime. Thus, high internal photoconductivity gain can be achieved in ZnO-nanowire devices.[13]

Figure 4b shows the transient response measured for the fabricated ZnO-nanowire phototransistor biased at a drain voltage of 5 V with the UV excitation (illuminated at 360 nm) switched on and off. It was found that the dynamic response of the ZnO-nanowire phototransistor was stable and reproducible with an on/off current contrast ratio of around 10^2. It was also found that the photocurrent increased rapidly when the UV excitation was turned on. In contrast, a slow response was observed when the UV light was turned off. The slow decay can probably be attributed to oxygen-related hole-trap states at the surface of the ZnO nanowire that prevent charge-carrier recombination. Figure 4c shows I_D-V_D characteristics of the device measured under illumination from the dispersed Xe arc lamp with a zero gate bias. It can be seen that the current in the fabricated device can be modulated efficiently by tuning the wavelength of the excitation. The proposed ZnO-nanowire phototransistor prepared on a glass substrate is thus potentially useful for low-cost mass-producible devices.

Figure 5a shows the measured low-frequency noise power spectra of the fabricated ZnO-nanowire phototransistor operated under various applied biases. The measured noise spectra can be fitted by the Hooge-type equation:[22]

$$S_n(f) = S_0 \frac{I_d^{\beta}}{f^{\alpha}} \tag{6}$$

where $S_n(f)$ is the spectral density of the noise power, S_0 is a constant, I_d is the dark current, and α and β are two fitting parameters. It can be seen that the low-frequency noise of the device was dominated by $1/f^2$ noise when the drain voltage was biased at 1−4 V. The exact reason for the deviation from standard noise is not yet known. It is possible that there exist spatially distributed interfacial trap states within the interface of the metal and ZnO nanowires. It is also possible that the deviation is related to the use of nanowires. Previously, it has been shown that the exponent α of metallic nanowires also deviates from 1 when the diameter of the nanowires is reduced.[23,24] Noise equivalent power (NEP) and normalized detectivity (D^*) are important parameters for evaluation of the phototransistor performance. For a bandwidth B, the total square noise current power can be estimated by integrating the noise spectral density over the frequency range:

$$\langle i_n \rangle^2 = \int_0^B S_n(f)\, df = \int_0^1 S_n(1)\, df + \int_1^B S_n(f)\, df$$
$$= S_0[\ln(B) + 1] \tag{7}$$

where $S_n(f)$ in the bandwidth range from 0 to 1 was assumed to be constant and equal to $S_0[S_n(f = 1\text{ Hz})]$. Thus, the NEP can be expressed as

$$\text{NEP} = \frac{\sqrt{\langle i_n \rangle^2}}{R} \tag{8}$$

where R is the responsivity of the phototransistor illuminated at 360 nm. D^* can then be determined using

$$D^* = \frac{\sqrt{A}\sqrt{B}}{\text{NEP}} \tag{9}$$

where A is the area of the phototransistor. According to eqs 8 and 9, for $B = 1000$ Hz, $A = 7.2 \times 10^{-10}$ cm^2, and a 360-nm light power = 1.1×10^{-3} W cm^{-2}, D^* and NEP as functions of the applied voltage can be obtained, as shown in Figure 5b. When the drain voltage was biased at 1 V, it was found that NEP and D^* of the fabricated ZnO phototransistor were 6.67×10^{-17} W and 1.27×10^{13} cm Hz$^{0.5}$ W^{-1}, respectively. It was also found that D^* decreased whereas NEP increased monotonically with the applied bias, which indicates that noise increases much faster than responsivity when the applied bias is increased. This suggests that the detectivity of the proposed phototransistor is limited by the bias-induced internal noise. Using molecular-beam epitaxy to grow the ZnO film, Chang et al. reported the fabrication of a 2D ZnO photoconductive sensor on a sapphire substrate with a NEP value of 1.83×10^{-6} W and a D^* value of 6.91×10^5 cm Hz$^{0.5}$ W^{-1}.[25] Compared with their results, the NEP value of the proposed phototransistor is significantly smaller, whereas the D^* value is significantly larger. The small NEP and large D^* suggest that the 1D ZnO-nanowire phototransistor reported in this study is potentially useful for UV light sensing.

IV. CONCLUSION

The fabrication of a phototransistor via the bridging of two prefabricated electrodes with a laterally grown ZnO nanowire was reported. It was found that the fabricated device is an n-channel enhancement-mode phototransistor with a dark carrier concentration of 6.34×10^{17} cm^{-3} when the gate voltage is biased at 5 V. With an incident-light wavelength of 360 nm and a zero gate bias, it was found that NEP and D^* values of the fabricated ZnO

phototransistor were 6.67×10^{-17} W and 1.27×10^{13} cm $Hz^{0.5}$ W^{-1}, respectively. It was also found that the current in the device can be modulated efficiently by tuning the wavelength of the excitation.

AUTHOR INFORMATION

Corresponding Author
*E-mail: tj.Hsueh@gmail.com.

ACKNOWLEDGMENT

This work was supported, in part, by the Center for Frontier Materials and Micro/Nano Science and Technology, National Cheng Kung University, Taiwan (Grant D97-2700). This work was also supported, in part, by the Advanced Optoelectronic Technology Center, National Cheng Kung University, under projects from the Ministry of Education.

REFERENCES

(1) Wu, J. J.; Liu, S. C. *Adv. Mater.* **2002**, *14*, 215–218.
(2) Park, W. I.; Jun, Y. H.; Jung, S. W.; Yi, G. C. *Appl. Phys. Lett.* **2003**, *82*, 964–966.
(3) Wei, C. S.; Lin, Y. Y.; Hu, Y. C.; Wu, C. W.; Shih, C. K.; Huang, C. T.; Chang, S. H. *Sens. Actuators A* **2006**, *128*, 18–24.
(4) Hsieh, H. H.; Wu, C. C. *Appl. Phys. Lett.* **2006**, *89*, 041109.
(5) Zhu, J.; Chen, Y.; Saraf, G.; Emanetoglu, N. W.; Lu, Y. C. *Appl. Phys. Lett.* **2006**, *89*, 103513.
(6) Kadota, M.; Nakao, T.; Murata, T.; Matsuda, K. *Jpn. J. Appl. Phys.* **2009**, *48*, 07GG03.
(7) Chang, S. P.; Chang, S. J.; Chiou, Y. Z.; Lu, C. Y.; Lin, T. K.; Lin, Y. C.; Kuo, C. F.; Chang, H. M. *J. Electrochem. Soc.* **2007**, *154*, J209–J211.
(8) Lee, K.; Kim, K. T.; Choi, J. M.; Oh, M. S.; Hwang, D. K.; Jang, S.; Kim, E.; Im, S. *J. Phys. D* **2008**, *41*, 135102.
(9) Bao, J. M.; Zimmler, M. A.; Capasso, F.; Wang, X. W.; Ren, Z. F. *Nano Lett.* **2006**, *6*, 1719–1722.
(10) Lin, Y. F.; Jian, W. B. *Nano Lett.* **2008**, *8*, 3146–3150.
(11) Huang, M. H.; Mao, S.; Feick, H.; Yan, H. Q.; Wu, Y. Y.; Kind, H.; Weber, E.; Russo, R.; Yang, P. D. *Science* **2001**, *292*, 1897–1899.
(12) Kind, H.; Yan, H. Q.; Messer, B.; Law, M.; Yang, P. D. *Adv. Mater.* **2002**, *14*, 158–160.
(13) Soci, C.; Zhang, A.; Xiang, B.; Dayeh, S. A.; Aplin, D. P. R.; Park, J.; Bao, X. Y.; Lo, Y. H.; Wang, D. *Nano Lett.* **2007**, *7*, 1003–1009.
(14) Lee, J. S.; Islam, M. S.; Kim, S. *Nano Lett.* **2006**, *6*, 1487–1490.
(15) Law, J. B. K.; Thong, J. T. L. *Nanotechnology* **2007**, *18*, 055601.
(16) Weng, W. Y.; Chang, S. J.; Hsu, C. L.; Hsueh, T. J.; Chang, S. P. *J. Electrochem. Soc.* **2010**, *157*, K30–K33.
(17) Kim, D. J.; Hyung, J. H.; Seo, D. W.; Suh, D. I.; Lee, S. K. *J. Electron. Mater.* **2010**, *39*, 563–567.
(18) Lind, E.; Persson, A. I.; Samuelson, L.; Wernersson, L. E. *Nano Lett.* **2006**, *6*, 1842–1846.
(19) Bae, H. S.; Im, S. *Thin Solid Films* **2004**, *469*, 75–79.
(20) Garrido, J. A.; Monroy, E.; Izpura, I.; Munoz, E. *Semicond. Sci. Technol.* **1998**, *13*, 563–568.
(21) Heo, Y. W.; Kang, B. S.; Tien, L. C.; Norton, D. P.; Ren, F.; La Roche, J. R.; Pearton, S. J. *Appl. Phys. A: Mater. Sci. Process.* **2005**, *80*, 497–499.
(22) Hooge, F. N.; Kedzia, J.; Vandamme, L. K. J. *J. Appl. Phys.* **1979**, *50*, 8087–8089.
(23) Bid, A.; Bora, A.; Raychaudhuri, A. K. *Nanotechnology* **2006**, *17*, 152–156.
(24) Dutta, P.; Horn, P. M. *Rev. Mod. Phys.* **1981**, *53*, 497–516.
(25) Chang, S. P.; Chang, S. J.; Chiou, Y. Z.; Lu, C. Y.; Lin, T. K.; Lin, Y. C.; Kuo, C. F.; Chang, H. M. *Sens. Actuators A* **2007**, *140*, 60–64.